Single Crystal Growth Technology of Room-temperature Compound Semiconductors for Radiation Detection and a role of the Radiation Equipment Fab. Center

Han Soo KIM*, Chang Goo KANG, Jang Ho HA, Jeong Min PARK, Young Soo KIM, Soo Jin KIM,
Korea Atomic Energy Research Institute, 29 Geumgu-gil, Jeongeup-si, Jeollabuk-do, Korea (56212)
**Corresponding author: khsoo@kaeri.re.kr*

1. Introduction

Detection of radiation is originated from the interaction of detection materials such as gas, scintillator, semiconductor, and so on. Most commercially available and deployed radiation detectors that provide a spectral response are based on either semiconductor or scintillation detection technologies. Among them, the current benchmarks for spectroscopic detection systems are based on high purity Ge (HPGe) semiconductor. But the drawback on HPGe detectors is that they need to be cooled to cryogenic temperatures in order to operation optimally due to the intrinsically low room temperature value of the Ge bandgap(0.67 eV). Many compound semiconductors with larger bandgaps, which enable operate at room temperature, have come under investigation as candidate materials for radiation detectors that identify and characterize sources as farther standoff distances and shorter measurement time. In this paper, currently used single crystal growth technologies of compound semiconductors for gamma-ray spectroscopy at room temperature are presented. And also a role of the radiation equipment fabrication center is addressed.

2. Current Room-temperature Compound Semiconductors for Radiation Detection (RTSD)

The key properties of consideration for designing a compound semiconductor to serve as a gamma-ray spectroscopy are density, atomic number, and the bandgap. Most elements from rows five and six of the periodic table exist as metals, so an additional element is needed to form an ionic-covalent compound with a bandgap wide enough to suppress thermal excitation of electrons. A bandgap between 1.5 eV ~ 2.5 eV is usually suitable for spectrometer applications at room temperature. A suitable detector should be able to exhibit a photopeak resolution of 1% or less at 500 keV gamma-ray energy with a volume of $1cm^3$ [1,2]. Another key properties include insulator level resistivity values, W-value, and charge carrier mobility lifetime products. To select and develop attractive materials for room temperature compound semiconductor radiation detector applications, it is important to optimize these three key properties.

2.1 CdTe compounds, TlBr, and HgI_2

Among all semiconducting compounds with attractive physical and electronic properties, CdTe and CdZnTe (CZT) are the forefront materials. It is common to alloy Zn into the crystal to increase after long periods under bias [3]. Today, the premier semiconductor material for ambient temperature radiation sensing applications is <15% Zn-doped CdTe, which features a bandgap around 1.57 eV (for 10% Zn-doped) at 300 K and resistivity improved 1–2 orders of magnitude over pure CdTe.91 With modern charge sensing and depth of interaction correction techniques, it is possible for CZT to exhibit photopeak resolution well below 1% at 662 keV [4-6].

Like most semiconductors, TlBr features some degree of bandgap trap states from point defects. Fortunately, the dominant defects are electrically neutral and pin the Fermi level near the middle of the bandgap that helps maintain high resistivity in the crystal. One of the other main drawbacks in TlBr historically has been polarization that leads to the degeneration of electronic performance after extended periods under bias.114 However, by engineering the crystals with Tl contacts, this issue has been solved. Currently, both pixelated and capacitive Frisch grid detectors have demonstrated a resolution of <1% at 662 keV [7,8].

The final product of the highly developed RTSD materials is HgI_2. Early attempts to produce gamma-ray spectra with HgI_2 proved challenging due to the hole's mobility lifetime product lagging orders of magnitude behind that of electrons. Due to this, the charge induced on an electrode from a gamma-ray interaction has a strong dependence on the location within the crystal where the interaction takes place. A remedy for this problem is found by engineering electrode geometries that allow electrons to induce the majority of charge from a radiation interaction. 1.55% resolution for the 662 keV gamma ray of ^{137}Cs by collecting charge from pixelated anode electrodes and performing depth correction on interaction signals was shown [9].

2.2 Emerging RTSD materials

Many of the emerging RTSD compounds have been identified by the dimensional reduction concept posed. These materials are mainly ionic and can be classified as either chalcogenides that are based on the anions S, Se, and Te or chalcohalides that are based on the anions Cl, Br, and I. Another RTSD materials are based on Pnictogenides, oxides, carbides, and organic hybrid

compounds. Electronic properties of these RTSD materials are shown in Table 1.

Table 1. Electronic properties of candidate RTSD materials [10]

Material	Bandgap (eV)	Resistivity (Ω cm)	$(\mu\tau)_e$ (cm^2/V)	Pair creation energy
CdTe	1.44	1×10^{9}	$1\text{–}2\times10^{-2}$	4.43
CdZnTe	1.57	$10^{9}\text{–}10^{10}$	7.5×10^{-3}	4.64
HgI_2	2.15	1×10^{13}	3×10^{-4}	4.20
TlBr	2.68	1×10^{10}	3×10^{-3}	6.50
CdMnTe	1.61	3×10^{10}	7×10^{-3}	2.12
CdSe	1.73	1×10^{12}	6.3×10^{-5}	5.50
CdZnSe	2.00	2×10^{10}	1×10^{-4}	6.00
CdTeSe	1.47	5×10^{9}	4×10^{-3}	(4.56)
GaAs	1.42	1×10^{8}	8×10^{-5}	4.20
GaSb	0.72	n.r.	3×10^{-5}	(2.51)
GaSe	2.03	$10^{8}\text{–}10^{10}$	3.7×10^{-5}	4.49
GaTe	1.66	1×10^{9}	n.r.	(5.08)
GaN	3.40	1×10^{11}	1×10^{-4}	10.2
GaP	2.26	1×10^{9}	1×10^{-5}	7.00
InP	1.34	1×10^{9}	5×10^{-6}	4.20
AlSb	1.65	1×10^{8}	1.2×10^{-4}	4.71
$TlHgInS_3$	1.74	4×10^{9}	3.6×10^{-4}	(5.30)
$Cs_2Hg_6S_7$	1.63	6×10^{7}	1.7×10^{-3}	(4.99)
$CsHgInS_3$	2.30	9×10^{10}	3.6×10^{-5}	(6.83)
$TlGaSe_2$	1.93	1×10^{9}	6×10^{-5}	(5.82)
$AgGaSe_2$	1.70	1×10^{11}	6.0×10^{-6}	(5.19)
$TlInSe_2$	1.10	$10^{6}\text{–}10^{7}$	1×10^{-2}	3.60
$LiInSe_2$	2.85	1×10^{11}	3.0×10^{-6}	(8.33)
$LiGaSe_2$	2.80	1×10^{8}	n.r.	(8.19)
$CsCdInSe_3$	2.40	4×10^{9}	1.2×10^{-5}	(7.10)
Tl_3AsSe_3	n.r.	$10^{6}\text{–}10^{7}$	n.r.	n.r.
$Cs_2Hg_3Se_4$	2.1	1.1×10^{9}	8.0×10^{-4}	(6.28)
$Pb_2P_2Se_6$	1.88	5×10^{11}	3.1×10^{-4}	(5.68)
$Cu_2I_2Se_6$	1.95	10^{12}	n.r.	(5.87)
$CsCdInTe_3$	1.78	2×10^{8}	1.1×10^{-4}	(5.06)
$Cs_2Cd_3Te_4$	2.5	1×10^{6}	1.1×10^{-4}	(7.38)
PbI_2	2.32	1×10^{13}	1×10^{-5}	4.90
InI	2.00	1×10^{11}	7×10^{-5}	(6.01)
SbI_3	2.20	1×10^{10}	n.r.	(6.56)
BiI_3	1.67	$10^{8}\text{–}10^{11}$	1×10^{-4}	5.80
β-$Hg_3S_2Cl_2$	2.56	1×10^{10}	1.4×10^{-4}	(7.54)
$CsPbBr_3$	2.25	$10^{9}\text{–}10^{11}$	1.7×10^{-3}	(6.69)
$Hg_3Se_2Br_2$	2.22	1×10^{11}	1.4×10^{-4}	(6.56)
SbSeI	1.70	1×10^{8}	4.4×10^{-4}	(5.19)
Tl_4CdI_6	2.80	2×10^{10}	6.1×10^{-4}	(8.19)
Tl_6SI_4	2.04	1×10^{10}	2.1×10^{-3}	(6.12)
Tl_6SeI_4	1.86	4×10^{12}	7.0×10^{-3}	(5.63)
Tl_4HgI_6	n.r.	$10^{11}\text{–}10^{12}$	8.0×10^{-4}	n.r.
$TlSn_2I_5$	2.14	4×10^{10}	1.1×10^{-3}	(6.39)
$Hg_3S_2I_2$	2.25	2×10^{11}	1.6×10^{-6}	(6.69)
$Hg_3Se_2I_2$	2.12	1.2×10^{12}	1.0×10^{-5}	(6.34)
$Hg_3Te_2I_2$	1.93	3.5×10^{12}	3.3×10^{-6}	(5.82)
LiZnAs	1.51	$10^{6}\text{–}10^{11}$	n.r.	(4.67)
LiZnP	2.04	$10^{6}\text{–}10^{11}$	n.r.	(6.12)
4H-SiC	3.27	2×10^{12}	4×10^{-4}	7.78
Diamond	5.47	5×10^{14}	2.7×10^{-7}	13.0
PbO	2.80	1×10^{13}	1×10^{-8}	(8.19)
ZnO	3.30	3×10^{13}	$10^{-6}\text{–}10^{-4}$	(8.37)
$MAPbI_3$	1.54	$10^{8}\text{–}10^{9}$	1.0×10^{-2}	(4.75)
$FAPbI_3$	1.43	$10^{6}\text{–}10^{9}$	1.8×10^{-2}	(4.40)
$FACsPb(BrI)_3$	1.52	$10^{8}\text{–}10^{9}$	1.2×10^{-1}	(4.69)
$MAPb(BrI)_3$	n.r.	n.r.	1.0×10^{-5}	n.r.
$MAPbBr_3$	2.3	1.7×10^{7}	1.2×10^{-2}	(6.83)
$MAPbBr_3$:Cl	2.3	3.6×10^{9}	1.2×10^{-2}	(6.83)

3. Single Crystal Growth Technologies of RTSD

Crystal growth of RTSD materials requires precise knowledge of the existence regions of the solid, liquid and gas phases with respect to temperature, pressure and composition. For this purpose, the temperature versus composition, T-x, component pressure or total pressure versus temperature, p-T or P-T, and finally p-T-x or P-T-x diagrams have been experimentally determined and theoretically modeled. Vertical or horizontal Bridgman method, Traveling Heater Method (THM), Zone Melting Method, and solution processing are currently used for single crystal growth of RTSD materials. First step is synthesis of compound components, which are almost above 6N purity. Bridgman method, which is using the temperature gradient to crystallization from the melts, is a basic crystal growing method. THM is using the component solution to attain the lower growth temperature, such as in case of CdZnTe growth in Te solution. Zone melting method is commonly used when grow a single crystal and purify the melts. Figure 1 and 2 show examples of a Bridgman and THM furnace. Figure 3 shows an example of a zone melting furnace and its crystal growth principle.

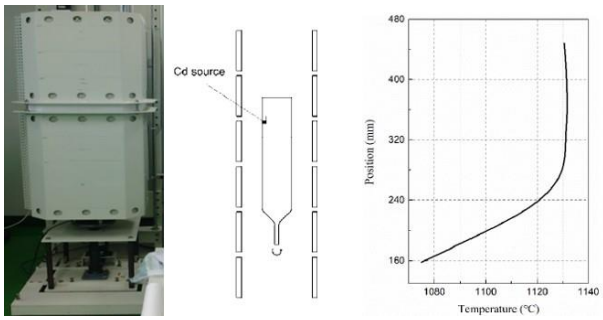

Figure 1. Bridgman furnace in KAERI and an example of temperature gradient

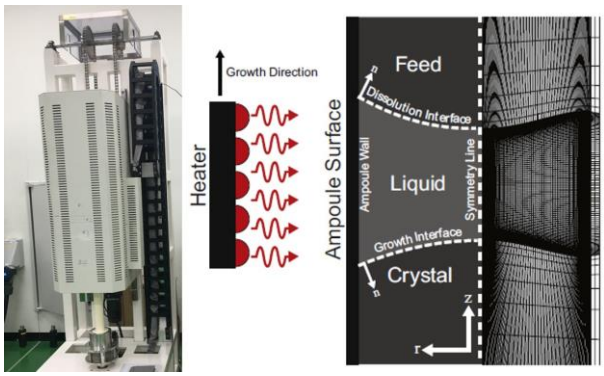

Figure 2. THM furnace in KAERI and principle of THM growth

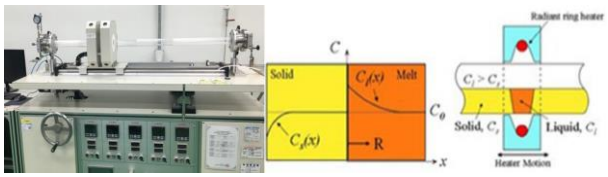

Figure 3. Zone Melting furnace in KAER and principle of zone melting crystal growth

4. A role of Radiation Equipment Fab. Center

Key Infrastructures of the Radiation Equipment Fab. Center are a crystal growth facility, a semiconductor fabrication process facility, an evaluation facility and a high energy X-ray & fast neutron facility. Currently development drifts of the Fab. Center are detection material development from scintillators to compound semiconductors and X- & gamma-ray detection sensor technologies. Supporting the Korean-style radiation equipment companies by utilizing the integrated radiation equipment infrastructure centering on the radiation equipment fab. Center is also an important role.

Figure 4 and 5 show the main facilities of the radiation equipment fab. center and major R&D related to single crystal growth, respectively.

Figure 4. Crystal growth facility (left) and semiconductor fabrication facility (right)

Figure 4. Crystal growth of compound semiconductor (left) and Scintillator (right) in KAERI

REFERENCES

[1] B. Obama, National strategy for Counterterrorism (US White House, 2011), vol. 28, p. 201, 2011.
[2] A. Owens, "Compound Semiconductor Radiation detectors, Taylor & Franancis, 2012.
[3] J.F. Butler, C. I., Lingren, and F. P. Doty, "CdZnTe gamma ray detectors," IEE Tans. Nucl. Sci., 39(4), P.605. 1992
[4] Q. Zhang et al., "Progress in the development of CdZnTe unipolar detectors for different anode geometries and data corrections," Sensors 13(2), p. 2447, 2013.
[5] A. E. Bolotnikov et al., "Use of high-granularity CdZnTe pixelated detectors to correct response non-uniformities caused by defects in crystals," Nucl. Instrum. Methods Phys. Res. A 805, p. 41. 2016.
[6] M. Streicher et al., "A portable 2 × 2 digital 3D CZT imaging spectrometer system,", 2014 IEEE Nuclear Science Symposium and Medical Imaging Conference (NSS/MIC), IEEE, 2014.
[7] H. Kim et al., "Continued development of thallium bromide and related compounds for gamma-ray spectrometers," Nucl. Instrum. Methods Phys. Res. A 629(1), p. 192, 2011.
[8] K. Hitomi et al., "TlBr capacitive Frisch grid detectors," IEEE Trans. Nucl. Sci. 60(2), p. 1156, 2013.
[9] J. E. Baciak and Z. He, "Comparison of 5 and 10 mm thick HgI2 pixelated ɣ -ray spectrometers," Nucl. Instrum. Methods Phys. Res. A 505(1–2), P. 191 (2003).
[10] Paul M. Johns and Juan C. Nino, "Room Temperature semiconductor detectors for nuclear security," J. Appl. Phys., 126, P. 126 (2019).